Capturing auxin response factors syntax using DNA binding models

Arnaud Stigliani[1], Raquel Martin-Arevalillo[1,2], Jérémy Lucas[1], Adrien Bessy[1], Thomas Vinos-Poyo[1], Victoria Mironova[3,4], Teva Vernoux[2], Renaud Dumas[1] and François Parcy[1,*]

1: Univ. Grenoble Alpes, CNRS, CEA, INRA, BIG-LPCV, 38000 Grenoble, France

2: Laboratoire de Reproduction et Développement des Plantes, Univ Lyon, ENS de Lyon, UCB Lyon1, CNRS, INRA, 46 allée d'Italie, F-69364, Lyon, France

3: Novosibirsk State University, Pirogova street 2, Novosibirsk, Russia

4: Institute of Cytology and Genetics SB RAS, Lavrentyeva avenue 10, Novosibirsk, Russia

*Contact: François Parcy Tel: +33 0438784978 Fax: +33 0438784091; Email: francois.parcy@cea.fr

ABSTRACT

Auxin is a key hormone performing a wealth of functions throughout the plant life cycle. It acts largely by regulating genes at the transcriptional level through a family of transcription factors (TF) called auxin response factors (ARF). Even if all ARF monomers analysed so far bind a similar DNA sequence, there is evidence that ARFs differ in their target genomic regions and regulated genes. Here we use position weight matrices (PWM) to model ARF DNA binding specificity based on published DNA affinity purification sequencing (DAP-seq) data. We find that the genome binding of two ARFs (ARF2 and ARF5/Monopteros/MP) differ largely because these two factors have different preferred ARF binding site (ARFbs) arrangements (orientation and spacing). We illustrate why PWMs are more versatile to reliably identify ARFbs than the widely used consensus sequences and demonstrate their power with biochemical experiments on the regulatory regions of the *IAA19* model gene. Finally, we combined gene regulation by auxin with ARF-bound regions and identified specific ARFbs

configurations that are over-represented in auxin up-regulated genes, thus deciphering the ARFbs syntax functional for regulation. This provides a general method to exploit the potential of genome-wide DNA binding assays and decode gene regulation.

Running title: Deciphering ARF DNA binding syntax

34 **INTRODUCTION**

35 Auxin is a key hormone in plants affecting multiple developmental processes
36 throughout the lifecycle of the plant. Most long-term developmental auxin responses
37 (such as embryo polarity establishment, tropisms, phyllotaxis or secondary root
38 emergence) involve modifications of gene expression by the nuclear auxin pathway
39 (Lavy and Estelle, 2016; Weijers and Wagner, 2016). This pathway includes a family
40 of transcription factors (TFs) called Auxin Response Factors (ARF) (Weijers and
41 Wagner, 2016; Leyser, 2018). In the absence of auxin, the Aux/IAA repressors bind
42 ARF TFs and form inactive multimers thereby preventing their activity (Han et al.,
43 2014; Korasick et al., 2015). The presence of auxin leads to the degradation of Aux/IAA
44 proteins and therefore allows ARFs to activate transcription.

45 ARF proteins exist in 3 classes (A, B and C) with class A corresponding to ARF
46 activators and B and C to ARF repressors (Finet et al., 2013). Understanding ARF
47 biochemical properties (DNA binding specificity, capacity to activate or repress
48 transcription, capacity to interact with partners) is important to decipher how different
49 tissues could respond differently to the same auxin signal (Leyser, 2018). ARFs are
50 modular proteins with several functional domains: most ARFs (except ARF3/ETTIN,
51 ARF17 and ARF23) have a PB1 domain (previously called domain III/IV) responsible
52 for interaction with the Aux/IAA repressors, TFs from other families and possible
53 homo-oligomerization through electrostatic head-to-tail assembly (Nanao et al., 2014;
54 Korasick et al., 2014; Parcy et al., 2016; Weijers and Wagner, 2016; Mironova et al.,
55 2017). ARFs also possess a DNA binding domain (DBD) from the plant specific B3
56 family. The structure of this DBD has been solved for ARF5 (also called
57 Monopteros/MP) and ARF1 revealing a B3 domain embedded within a flanking
58 domain (FD) and a dimerization domain (DD) (Boer et al., 2014). The DD allows ARF
59 proteins to interact as a face-to-face dimer with a DNA element called an everted repeat
60 (ER) made of two ARF binding sites (ARFbs). ARFbs have been originally defined as
61 TGTCTC (Ulmasov et al., 1995; Guilfoyle et al., 1998) and this knowledge was used
62 to construct a widely used auxin transcriptional reporter, DR5 (Ulmasov et al., 1997).
63 More recently, Protein Binding Microarray (PBM) experiments suggested that
64 TGTCGG are preferred ARFbs and a new version of DR5, DR5v2, was built based on
65 this cis-element (Boer et al., 2014; Franco-Zorrilla et al., 2014; Liao et al., 2015). ARFs

66 are able to bind different ARFbs configurations in addition to ER such as direct repeats
67 (DR) or, as recently suggested, inverted repeats (IR) (O'Malley et al., 2016). Whether
68 ARF oligomerization through the PB1 domain contributes to binding of some ARFbs
69 configurations such as IR or DR that are not compatible with DD dimerization has been
70 proposed but not yet demonstrated (O'Malley et al., 2016; Parcy et al., 2016). Based on
71 affinity measurements of interaction between ARF DBD (for ARF1 and MP) and a few
72 ER cis-elements, it was proposed that ARFs differ by the type of ER configuration they
73 prefer: the ARF1 repressor has a much narrower range of preferences than the MP
74 activator (this was called the molecular caliper model) (Boer et al., 2014). However,
75 this model was established using isolated ARF DBD lacking the PB1 domain and did
76 not include interaction with DR and IR ARFbs configurations.

77 Despite the central importance of ARF TFs, models reliably predicting their DNA
78 binding specificity are still scarce (Keilwagen et al., 2011; Mironova et al., 2014) and
79 simple consensus sequences are often used (Berendzen et al., 2012; O'Malley et al.,
80 2016; Zemlyanskaya et al., 2016) that hardly capture possible sequence variation within
81 the cis-element. Recently, DNA affinity purification sequencing (DAP-seq) data have
82 offered a genome-wide view for two full-length ARF proteins of Arabidopsis (the
83 repressor ARF2 and the activator MP) (O'Malley et al., 2016). The DAP-seq assay is
84 technically similar to ChIP-seq but with chromatin-free isolated genomic DNA and
85 with a single recombinant protein added. Based on TGTC consensus sequence as
86 ARFbs definition, the MP activator and the ARF2 repressor appear to have different
87 preferred DNA binding sites. They share a novel inverted repeat (IR7-8) element but
88 also have specific binding sites with different spacing and orientation of ARFbs
89 (O'Malley et al., 2016). Here we undertook an extensive reanalysis of DAP-seq data
90 using position weight matrix (PWM) as the DNA binding specificity model
91 (Wasserman and Sandelin, 2004). PWMs represent a simple but efficient tool that
92 captures the base preference at each position of the motif. PWMs give a score to any
93 DNA sequence with zero for the optimal sequence and more negative scores as the
94 sequence diverges from the optimum. The PWM score is then a quantitative value
95 directly related to the affinity of the DNA molecule for the protein (Berg and von
96 Hippel, 1987). Using PWMs, we establish differences between ARF2 and MP and show
97 that they reliably identify a binding site syntax explaining their specificity. We further

98 illustrate the predictivity of PWM as compared to consensus using binding assays and
99 identify ARFbs configurations enriched in promoters of genes regulated by auxin.

100 **RESULTS**

101 **ARF2 and MP have similar DNA binding sites but bind different genome regions**

102 Using the published DAP-seq data (O'Malley et al., 2016), we first compared the sets
103 of genomic regions bound by ARF2 and MP. Two regions were considered bound by
104 both factors when they overlapped by at least 50% (see Methods). As expected for two
105 TFs from the same family, there is a significant overlap and many regions are bound
106 by both factors (Figure 1A). However, the large number of regions specifically bound
107 by only one of them indicates a clear difference between ARF2 and MP DNA binding
108 preferences (Figure 1A). This remains true even when focusing on regions bound with
109 the highest confidence (top 10%, see Methods) by each of the factors (Supplemental
110 Figure 1). We intended to explain these differences by characterizing ARF2 and MP
111 DNA binding specificity. The examination of the DNA motif logo derived from regions
112 recognized by ARF2 or MP monomers revealed only minor differences (Figure 1C).
113 For both logos, the G[4] position corresponding to a direct protein-base contact in the
114 ARF1 structure (Boer et al., 2014) is highly invariant. At positions [7,8] where the
115 original ARFbs harboured TC (Guilfoyle et al., 1998), the preferred sequence is GG as
116 recently proposed from PBM experiments (Boer et al., 2014; Franco-Zorrilla et al.,
117 2014) but this preference is not as pronounced as in PBM-derived logos and sequence
118 variations at these positions is tolerated.

119 We built ARF2 and MP PWMs to model their DNA binding. We evaluated the
120 prediction power of each PWMs using Receiver Operating Characteristics Area Under
121 the Curve analysis (ROC-AUC or AUROC) (Hanley and McNeil, 1982) based on the
122 ARFbs of best score present in each bound region (Figure 1B). Such analysis yields an
123 AUROC value of 1 for a perfect model and 0.5 for a model with no predictive value.
124 This analysis requires the generation of a negative set of regions for comparison. For
125 this, we improved a previously designed tool, a negative set builder (Sayou et al., 2016),
126 to extract from the Arabidopsis genome a set of non-bound regions with similar features
127 as bound ones (size, GC content, genomic origin – see Methods). Based either on the
128 full set of bound regions (Figure 1B) or only the 10% top ranked regions (Supplemental

Figure 1), we found that MP model is highly predictive (AUROC= 0.84) while ARF2's has a lower performance (AUROC= 0.69).

PWM models assume an additive contribution of each nucleotide position, a hypothesis that is not always true (Bulyk, 2002; Moyroud et al., 2011; Zhao et al., 2012; Mathelier and Wasserman, 2013). We used Enologos (Workman et al., 2005) to test for the presence of dependencies between some of the positions, particularly for positions [7,8] (Figure 1C) where mostly GG and TC doublets have been proposed so far. Enologos did not detect any dependency (Supplemental Figure 1) indicating that standard PWM can be adequately used. We also wondered whether the small differences between ARF2 and MP PWMs (as visible on their logos from Figure 1C) could contribute to their binding specificity. We thus tested the MP PWM on ARF2 regions and, conversely, ARF2 PWM on MP regions. The performance is indeed slightly weaker showing there is some specificity in the monomer PWM (Supplemental Figure 1). However, the very small difference suggests there must be other parameters explaining ARF2 and MP different specificities.

ARF2 and MP prefer different binding site configurations

Published analyses (O'Malley et al., 2016) suggested that MP and ARF2 might differ in their preferred ARFbs dimeric configurations (ER, DR or IR, Figure 2A). We thus analysed the distribution of spacings between ARFbs using PWM models. To do this, a score threshold needs to be chosen above which transcription factor binding site (TFBS) are considered. As this threshold cannot be experimentally determined, we performed the analysis within a range of scores (from -8 to -13, -8 being of better affinity than -13). We studied the overrepresentations of all dimer configurations (DR, ER and IR) as compared to a negative set of regions. Overall, DR, ER and IR are more frequent in the ARF bound regions than in the negative set (Figure 2B, left panel), consistent with the higher density of ARFbs in these regions. We next estimated the overrepresentation of each particular configuration (ERn, DRn or IRn with the spacing n varying between 0 and 30 bp) within the whole population of configurations and normalized it to the equivalent parameter in the negative set of regions (Figure 2). For example, if, for a given value of n, DRn represents 10% of all configurations (ER/DR/IR with $0 \leq n \leq 30$) in the positive set and only 2% in the negative one, DRn enrichment will be 5-fold.

161 This analysis revealed a striking difference between ARF2 and MP. For ARF2, ER7-8
162 are the only overrepresented configurations whereas MP showed a wider range of
163 preferred distances and configurations including DR4-5, DR14-15-16, DR25-26, ER7-
164 8, ER17-18, IR0, IR3, IR12-13, IR23-24 (Figure 2B). Our results contrast with
165 O'Malley's where IR8 was the most overrepresented configuration for both factors
166 (O'Malley et al., 2016). Since their result was obtained using a TGTC consensus as
167 ARFbs definition, we repeated our analysis with TGTC (Supplemental Figure 2A). We
168 still validated our result suggesting O'Malley et al. likely confused ER and IR. The MP
169 graph (Figure 2B) suggests a periodicity of overrepresented distances every 10 bp, a
170 hypothesis we confirmed by extending the distance window, revealing this trend for
171 MP but not for ARF2 (Supplemental Figure 2B). Modelling of DR5 and IR13
172 protein/DNA complexes structures based on ARF1 crystallographic data (PDB entry
173 4LDX) clearly illustrates that these configurations are incompatible with the
174 dimerization mode described for ER7 and could involve a different dimerization
175 interface (Figure 2D).

176 **ARF2 and MP have different DNA binding syntax**

177 We re-examined the Venn diagram from Figure 1A in the light of the identified
178 preferred configurations. We separated ARF2 and MP bound regions in three sets:
179 ARF2 specific, MP specific, ARF2/MP common regions. Because the two PWMs are
180 very similar, we used the ARF2 matrix and performed the same analysis as in Figure 2
181 but on the three sets of regions (Supplemental Figure 3). DR4/5/15 and IR0/13 are
182 overrepresented only in MP specific regions, ER7 in ARF2 specific regions and ER7/8
183 mostly in the MP/ARF2 common regions. Remarkably, MP-specific regions are even
184 depleted in ER7/8 compared to the negative set of sequences because these elements
185 are bound by both ARF2 and MP (Supplemental Figure 3). Plotting the frequency of a
186 few selected configurations illustrates the group specific characteristics (Figure 3). We
187 also used RSAT (Medina-Rivera et al., 2015) to search for other sequence features that
188 could distinguish the three groups of regions. For ARF2-bound regions only, we found
189 an enrichment for nine long AT-rich motifs similar to the one shown in Figure 3B.
190 These motifs are found all along the bound regions (not shown). One example of
191 enrichment of such a motif is illustrated in Figure 3B.

192 **Comparison between improved PWM models and consensus**

193 We incorporated the ARF2 and MP specific features in new PWM-based models and
194 tested their prediction power using AUROC. The improvement is marginal for MP but
195 better for ARF2 (Figure 4C, AUROC for monomeric ARF2bs = 0.69, for ER7/ER8
196 model = 0.74). To illustrate the fundamental differences between PWM and consensus,
197 we plotted the specificity (false positive rate) and sensitivity (true positive rate)
198 parameters on the PWM ROC curve (Figure 4). For the monomeric ARFbs models, the
199 TGTC consensus is poorly specific with almost 70% false positive rate. Conversely,
200 TGTCGG or TGTCTC perform correctly but leave no freedom in terms of sensitivity
201 and specificity: only the quantitative model allows to choose these parameters by
202 adjusting the score threshold. For ARF2 ER7/8 dimeric models, using any of the three
203 consensus is extremely stringent and detects very few sites in the positive set (at best
204 2.5% for TGTC) whereas the PWM model is again more versatile as it allows reaching
205 the desired specificity/sensitivity combination by adjusting the score threshold.

206 DNA binding models are extremely useful to detect transcription factor binding
207 site and challenge their role *in vitro* or *in vivo*. To scan individual sequences, PWMs
208 are superior as they provide a quantitative information linked to TFBS affinity (Berg
209 and von Hippel, 1987) and allow the detection of possible non-consensus sites of high
210 affinity. We used our models to identify binding sites on the well-studied promoter of
211 the *IAA19* gene ((Pierre-Jerome et al., 2016) and references therein). Scanning the
212 *IAA19* promoter sequence with ARF2 and MP PWMs identified several ARFbs (Figure
213 5) including a high-scoring ER8 site bearing one non-canonical gGTCGG that lacks the
214 TGTC consensus (Figure 5A). This site is located at the centre of a DAP-seq peak for
215 MP and ARF2. We tested ARF binding to this particular ER8 element and tested the
216 impact of the consensus presence on binding to ARF. For this, we restored the TGTC
217 consensus for this non-canonical ER8 element and also created an artificial ER8 that
218 has both TGTC consensus but suboptimal bases in other positions according to the
219 PWM (Figure 5B). Strikingly, the optimised PWM score better predicts the binding
220 than the presence of the consensus sequence: we observed intense binding on the non-
221 canonical ER8, only a slight improvement when the consensus is restored and no
222 binding on a consensus-bearing ER8 of low score (Figure 5C).

223 **PWM models reveal preferred ARFbs configurations in auxin regulated genes**

224 We next tested the PWM models on *in vivo* data. ChIP-seq data are available for ARF6
225 and ARF3 (Oh et al., 2014; Simonini et al., 2017). However, no obvious ARFbs could
226 be identified in any of these datasets. Testing ARFbs monomeric or dimeric models
227 yielded a very poor AUROC value (0.61 for ARF6 and 0.58 for ARF3) suggesting that
228 these data might not be adequate to evaluate our model. We also used the auxin
229 responsive genes datasets derived from a meta-analysis of 22 microarray data (see
230 Methods). We defined 4 groups of regions of either auxin induced or repressed genes
231 with high or very high confidence (very-high confidence: 153 up regulated genes, 36
232 down regulated; high confidence: 741 up regulated, 515 down regulated, Supplemental
233 File). We first analysed the 1500 bp promoters of the regulated genes compared to
234 unregulated ones. This analysis revealed a mild but detectable over-representation of
235 ER8 in up-regulated promoters (Supplemental Figure 4) as compared to unregulated
236 ones and nothing in down-regulated genes.

237 Next, we tested whether more information could be extracted from these promoters if
238 only the DNA segments bound by ARF in DAP-seq were analysed. We focused on
239 auxin-induced genes and regions bound by the MP activator ARF because the
240 mechanism of gene induction by auxin is well understood, while repression by auxin
241 and the role of repressor ARFs such as ARF2 is less clear. We therefore compared MP-
242 bound regions present in regulated versus non-regulated promoters. We observed that
243 the over-representation of ER8 and IR13 is higher in auxin upregulated genes than in
244 non-regulated ones (Figure 6A-B). This is particularly striking for the high-confidence
245 auxin induced genes even if this list likely also contains indirect ARF targets (Figure
246 6A). We tested MP binding to the IR13 probe and observed a strong and well-defined
247 MP/IR13 complex (Figure 6C), similar to those obtained with ER7/8 probes. The IR0
248 element, also enriched in MP-bound DAP-seq regions but not in auxin-regulated
249 promoters, gives a weaker smeary band. For auxin repressed genes, two configurations
250 (ER18 and IR3) are more overrepresented in the MP-bound regions from promoters of
251 downregulated genes than for non-regulated genes (Supplemental Figure 5). This might
252 indicate that some ARFbs configurations could be involved in repression by auxin but
253 this attractive hypothesis clearly requires to be tested with additional experiments.

254 **DISCUSSION**

255 **PWM versus consensus for auxin responsive elements**

256 A key question in auxin biology is how the structurally simple molecule evokes such
257 diverse responses. Transcription Factors of the ARF family are the main contributors
258 that diverge auxin response. Predictive tools to infer the presence of ARF binding sites
259 in regulatory regions are essential both for functional and evolutionary analyses. Most
260 studies so far have used TGTC-containing consensus sequences as a tool to detect
261 ARFbs (Berendzen et al., 2012; O'Malley et al., 2016; Zemlyanskaya et al., 2016). Here
262 we built PWM-based models and showed that they provide a greater versatility than
263 consensus sequences as they allow adjusting sensitivity and specificity. Even if a TGTC
264 consensus is perfectly suitable to detect the over-representation of some configurations
265 (such as ER7-8 for ARF2 and MP)(O'Malley et al., 2016) (Supplemental Figure 2), it
266 cannot be used to search regulatory regions because of its lack of specificity when used
267 as monomer and its extremely low sensitivity when used as ER7/8 dimer (Figure 4).
268 We illustrated on a chosen example (the *IAA19* promoter) that a site can be bound
269 without a TGTC consensus and not necessarily bound even when the consensus is
270 present (Figure 5). The non-canonical ER8 site we detected was challenged and
271 functionally validated by studies in yeast (Pierre-Jerome et al., 2016).

272 Even if more elaborate models exist (Mathelier and Wasserman, 2013), PWM have
273 emerged as the simplest and most performant models. Still, we were surprised that, in
274 a DAP-seq context where no other parameters (such as cofactors, histones or chromatin
275 accessibility) should influence TF/DNA binding, the PWM models could not reach
276 better AUROC values especially for ARF2. We have tried models that integrate the
277 DNA shape feature (Mathelier and Wasserman, 2013) but they did not significantly
278 improve the prediction power (data not shown). The newly identified sequences with
279 stretches of As and Ts (Figure 3B) were not easy to integrate in improved models but
280 might affect the overall context of ARF2 binding sites and contribute to ARF2 specific
281 regions. This finding is reminiscent of the family of AT-rich motifs found as
282 overrepresented in promoters of auxin responsive genes (Cherenkov et al., 2018). These
283 elements were mostly found in ARF2-binding regions and they were more associated
284 with down-regulation than with up-regulation. More studies are needed to elucidate
285 their role.

286 **ARF2 versus MP**

287 ARFs exist as activators and repressors (Dinesh et al., 2016). Affinity measurements
288 on a few DNA sequences *in vitro* (the molecular caliper model) and consensus-based
289 search in genome-wide binding data both indicate that activator ARF MP and repressor
290 ARF (ARF1 and ARF2) might have different preferences for ARFbs configurations
291 (Boer et al., 2014; O'Malley et al., 2016). But one study examined only a few ER
292 elements (Boer et al., 2014) whereas the other did not recover the long known ER7/8
293 elements and instead proposed IR7/8 (O'Malley et al., 2016). Using PWM-based
294 models and re-analysing DAP-seq data, we confirmed that MP and ARF2 have a similar
295 monomeric binding site but differ in the syntax of binding sites (combinations of
296 binding sites of ARF monomers) they recognize: ARF2 prefers ER7/8 while MP has a
297 much wider range of preferences. For ER motifs (face to face DBDs), our results extend
298 the molecular caliper model (Boer et al., 2014) at the genome-wide level with some
299 larger spacings. Moreover, MP has wider syntax than ARF2 as it also includes enriched
300 DR and IR motifs. Such findings cannot be accommodated with the molecular caliper
301 model as they involve different orientations of the two DBDs than in ER (head to tail
302 for DR and tail to tail for IR). As previously reported (O'Malley et al., 2016), MP shows
303 an increased binding frequency every 10 bp for all DR, ER and IR enriched
304 configurations. Because this spacing corresponds to a DNA helix turn, we can imagine
305 that this configuration allows interaction between ARF proteins on the same side of the
306 DNA. 3D modelling using the published ARF1 structure indicates that these
307 interactions are unlikely to involve the same dimerization surface as for ARF1 (Figure
308 2D). The proximity of some ARF DD domains in 3D, combined with possible
309 flexibility of ARF DBD suggest that these proteins might have evolved different
310 dimerization modes with the same protein domain. Confirming this hypothesis will
311 await their structural characterisation. An alternative hypothesis is that the PB1
312 oligomerization domain contributes to stabilize the MP binding to preferred motifs but
313 this also remains to be tested. However, it should be also noted that a preference for 10-
314 bp spaced binding sites does not necessarily implies the presence of protein-protein
315 contacts. Indeed, it has been shown that the binding of a first protein in the DNA major
316 groove favours the binding of a second one at a 10 bp distance through allosteric
317 changes in DNA conformation (Kim et al., 2013). This mechanism could also be at
318 work for ARF DNA binding.

319 It is interesting to note that ER7-8 is bound by both ARF2 and MP whereas some
320 configurations such as DR5 or IR13 are more specific to MP. If repressor ARFs act by
321 competing with activator ARFs for ARFbs (as proposed in Vernoux et al., 2011), this
322 competition will therefore depend on the nature of ARFbs (shared between activators
323 and repressors or specific to only one class of ARFs) . Some sites such as DR5 might
324 be less subjected to competition therefore influencing their activity as reporter for
325 auxin-dependent transcriptional activity (Ulmasov et al., 1997; Liao et al., 2015).
326 Extending this type of analysis to all members of the ARF family should indicate
327 whether ARF from a given class (A, B or C) (Finet et al., 2013) have a stereotypic
328 behaviour or whether there is also a diversity of properties within the class A ARF, for
329 example. Such differences would help explaining how a single auxin signal can trigger
330 different responses depending on the cell type where it is perceived (provided different
331 cell types express different sets of ARF proteins). *In vivo*, other parameters will also
332 play an important role for the response to auxin such as the ARF interaction partners
333 (Mironova et al., 2017) and chromatin accessibility.

334 **ARF binding versus auxin regulation**

335 The analysis of auxin-induced genes using PWM models identified only a small over-
336 representation of ER8 (Supplemental Figure 4), a motif shared by ARF2 and MP. As
337 we anticipated that ARFbs might be diluted in whole promoter sequences, we collected
338 the set of DNA regions present in promoters from auxin-induced genes that are also
339 bound by MP in DAP-seq and compared it to MP-bound promoter regions from non-
340 auxin-regulated genes. This analysis confirmed the overrepresentation of ER8 in auxin-
341 induced genes but also identified IR13 as enriched motifs (Figure 6). IR13 is a novel
342 element, well bound by MP *in vitro* that now requires *in planta* characterization. It is
343 not enriched in ARF2-bound regions suggesting it will likely be insensitive to
344 competition by repressor ARF2. We also characterized auxin repressed gene. Whether
345 repression directly involves ARFs is not known. Promoter analysis did not reveal any
346 motif enrichment but the intersection with MP-bound regions showed ER18 and IR3
347 over-representation (Supplemental Figure 5). Again, functional analysis of such motifs
348 *in planta* will be important in the future. We anticipate that the strategy we designed
349 here (combining DAP-seq data with expression studies) is a very general method to
350 increase the signal/noise ratio in regulatory regions and better detect binding sites

351 involved in regulation. DAP-seq is a powerful technique but it suffers from giving
352 access to DNA that might never be accessible in the cell. The combination with
353 differential expression studies (+/- a stimulation or +/- a TF activity) will be a powerful
354 way to narrow down the number of regions examined and extract functional regulatory
355 information.

356 **METHODS**

357 **Bio-informatic analyses**

358 The TAIR10 version of Arabidopsis genome was used throughout the analyses. The
359 DAP-seq peaks were downloaded from http://neomorph.salk.edu/PlantCistromeDB.
360 We sorted the peaks (200 bp) extracted from narrowPeaks file accordingly to their Q-
361 value. An ARF2-bound region was considered to overlap with an MP-bound region if
362 the overlap exceeded 100 bp. We used the Bedtools suite to assess the overlaps and
363 retrieve genome sequences. The PWM were generated using MEME Suite 4.12.0
364 (Bailey et al., 2009) on the 600 top peaks of ARF2 and MP according to the Q-value.

365 ROC-AUC analysis: performing a ROC analysis requires a background set of unbound
366 genomic regions. This set was built with a Python script that takes a *bed* file of bound
367 genomic regions as input and randomly selects in the Arabidopsis genome regions of
368 same size, similar GC content and with similar origin (intron, exon or intergenic).

369 To search for dependencies between positions of the ARF PWM, we used the sequence
370 alignment inferred by MEME Suite (Bailey et al., 2009) to build a PWM and used it as
371 input for Enologos selecting the option "mutual info" (Workman et al., 2005).

372 Analysis of ARFbs configurations

373 The absolute enrichment (A) for each type of configuration (DR, ER, IR) was calculated
374 as the ratio between the total number of sites in each configuration C in the bound set
375 of regions divided by the same number in the background set. Such calculations were
376 done for different score thresholds and normalized by the ratio between the total number
377 of monomeric sites (BS, with no threshold applied) in the foreground and in the
378 background to account for the different sequence sizes of the two sets. S_{max} stands for the
379 maximum spacing.

380 $$A_{C=DR,ER,IR} = \frac{\sum_{i=0}^{S_{max}} C_{i_{pos}}}{\sum_{i=0}^{S_{max}} C_{i_{neg}}} \cdot \frac{\sum BS_{neg}}{\sum BS_{pos}}$$

381 For the normalized enrichment, we inventoried all the dimer configurations made of
382 two monomeric ARFbs with scores above the chosen threshold. We then calculated the
383 frequency (f) of each particular conformation (DRn, ERn or IRn with $0 \leq n \leq S_{max}$) among
384 all dimeric sites in the positive set of bound regions and in the background set.

385 $$f_{i,C=DR,ER,IR} = \frac{C_i}{\sum_{\substack{k=0 \\ C=DR,ER,IR}}^{S_{max}} C_k}$$

386 The normalized enrichment (*N*) shown in figure 2 corresponds to the ratio between
387 frequencies in the positive set and in the negative set for a given spacing.

388 $$N_{i,C=DR,ER,IR} = \frac{f_{i,c_{pos}}}{f_{i,c_{neg}}}$$

389 To illustrate the enrichment of a few chosen motifs (DR4-15, ER7-8, IR0-13), we
390 identified all sequences displaying a potential binding site with a score higher than a -
391 8 threshold. Next, we plotted the % of regions displaying a given motif in the Venn
392 diagram regions. The same was done for AT-rich motifs with a score threshold for each
393 AT-rich PWM of a score -10.

394 The ER7/ER8 PWM for ARF2 was built from the ARF2 monomer PWM. Both ARF2
395 bound and unbound sets of regions were scanned with these two PWM and the best
396 score given to each region by either ER7 or ER8 was used to plot the ROC curve. For
397 the analysis of specificity and sensitivity of TGTC-containing consensus sequences, we
398 analysed each region for the presence or absence of ER7 or ER8 consensus (TGTCNN-
399 7/8N-NNGACA, TGTCGG-7/8N-CCGACA, TGTCTC-7/8N-GAGACA). A region
400 was scored positive when containing at least one site.

401 For the analysis of auxin regulated promoters, we used 1500 bp upstream of the first
402 exon of each gene. All DAP-seq regions overlapping with the promoters were then
403 selected for analyses.

404 The major scripts used are available on github: https://github.com/Bioinfo-LPCV-RDF.
405 The frequency matrices used to infer PWM can be downloaded on
406 https://github.com/Bioinfo-LPCV-RDF/Scores.
407
408 Selection of auxin regulated genes

409 We selected auxin regulated genes over twenty-two publicly available gene expression
410 profiling datasets from the GEO database (Supplemental File 1). The datasets were
411 generated on seedlings or roots of *A. thaliana* with different auxin concentrations and
412 times of exposure to auxin (explored in Zemlyanskaya et al., 2016). Differentially
413 expressed genes were defined as those expressed at least 1.5 times higher (lower) after
414 auxin treatment comparing to control, with FDR adjusted p-value < 0.05 (Welch t-test
415 with Benjamini-Hochberg correction). We compiled four groups of auxin-regulated
416 genes: induced or repressed genes with high or very high confidence (Supplemental
417 File 1). High confidence genes: 741 auxin up-regulated and 515 down-regulated genes
418 significantly (more than 1.5-fold, FDR adjusted $p < 0.05$) changed their expression after
419 auxin treatment in two or more datasets. Very high confidence genes: 153 auxin up-
420 regulated and 36 down-regulated genes significantly changed their expression in four
421 or more datasets.
422
423 **Expression and purification of recombinant proteins**
424 ARF2 and ARF5 coding sequences were cloned into pHMGWA vectors (Addgene)
425 containing N-terminal His-MBP-His tags. His-MBP-His-tagged ARF proteins were
426 expressed in *E. coli* Rosetta2 strain. Bacteria cultures were grown in liquid LB medium
427 to an $O.D_{600\ nm}$ of 0.6-0.9. Protein expression was induced with isopropyl-β-D-1-
428 thyogalactopiranoside (IPTG) at a final concentration of 400 μM. Protein production
429 was done overnight at 18 ºC. Bacteria cultures were centrifuged and the resulting pellets
430 were resuspended in Lysis buffer (Tris-HCl 20 mM pH 8; NaCl 500 mM; Tris(2-
431 carboxyethyl) phosphine (TCEP) 1 mM for ARF2 and Tris-HCl 20 mM pH 8; NaCl
432 500 mM; EDTA 0.5 mM; PMSF 0.5 mM; TCEP 1 mM; Triton 0.2 % (w/v) for ARF5)
433 with EDTA-free antiprotease (Roche) for sonication. Proteins were separated from the
434 soluble fraction on Ni-sepharose columns (GE Healthcare) previously equilibrated with
435 the corresponding Lysis buffer. Elutions were done with Imidazole 300 mM diluted in
436 the corresponding Lysis buffer.

437

438 **Electrophoretic Mobility Shift Assays (EMSAs)**

439 DNA-protein interactions were characterized by EMSAs. ER8 binding site was isolated
440 from Arabidopsis *IAA19* promoter and ER8 variant sequences are given in
441 Supplemental Table 1. IR0 and IR13 sequences were artificially designed with
442 TGTCGG consensus sites (Supplemental Table 1). EMSA DNA probes were prepared
443 from lyophilized oligonucleotides corresponding to the sense and antisense strands
444 (Eurofins). Oligonucleotides for the sense strand presented an overhanging G in 5' for
445 DNA labelling. Sense and antisense oligonucleotides were annealed in Tris-HCl 50
446 mM; NaCl 150 mM. The annealing step was performed at 98 °C for 5 minutes, followed
447 by progressive cooling overnight. Annealed oligonucleotides, at a final concentration
448 of 200 nM, were incubated at 37 °C for 1 hour with Cy5-dCTP (0.4 μM) and Klenow
449 enzyme in NEB2 buffer (New England Biolabs). The enzyme was inactivated by a 10-
450 minutes incubation at 65 °C. Oligonucleotides were conserved at 4 °C in darkness.
451 EMSAs were performed on agarose 2 % (w/v) native gels prepared with Tris-Borate,
452 EDTA (TBE) buffer 0.5 X. Gels were pre-run in TBE buffer 0.5 X at 90 V for 90
453 minutes at 4 °C. Protein-DNA mixes nonspecific unlabelled DNA competitor (salmon
454 and herring genomic DNA, Roche Applied Science; final concentration 0.045 mg/ml)
455 and labelled DNA (final concentration 20 nM) in the interaction buffer 25 mM HEPES
456 pH 7.4; 1 mM EDTA; 2 mM MgCl2; 100 mM KCl; 10% glycerol (v/v); 1 mM DTT;
457 0.5 mM PMSF; 0.1% (w/v) Triton. Mixes were incubated in darkness for 1 hour at 4°C
458 and next loaded in the gels. Gels were run for 1 hour at 90 V at 4 °C in TBE 0.5 X
459 DNA-protein and bindings were visualized on the gels with Cy5-exposition filter
460 (Biorad ChemiDoc MP Imaging System).

461 **AUTHOR CONTRIBUTION**

462 FP and RD designed and supervised the project, AS, JL, AB and VM performed the
463 bioinformatic analyses, RMA and TVP performed the biochemical experiments, all
464 authors discussed the results, FP wrote the manuscript with the help of AS, RD, TV,
465 RMA and VM.

466 **ACKNOWLEDGEMENTS**

We thank Anthony Mathelier for discussions, Line Andresen and Chloe Zubieta for critical reading of the manuscript and David Mast and Laura Grégoire for implication in early stage of this work.

FUNDING

This work was supported by the Agence Nationale de la Recherche [ANR-12-BSV6-0005 Auxiflo to RD, TV, FP], a PhD fellowships from the University Grenoble Alpes [RAM], the Grenoble Alliance for Cell and Structural Biology [ANR-10-LABX-49-01 to FP, RD, AS], Russian State Budget [0324-2018-0019 to VM] and Russian Foundation for Basic Research [18-04-01130 to VM]

CONFLICT OF INTEREST

We declare no conflict of interest

REFERENCES

Bailey, T. L., Boden, M., Buske, F. A., Frith, M., Grant, C. E., Clementi, L., Ren, J., Li, W. W., and Noble, W. S. (2009). MEME SUITE: tools for motif discovery and searching. *Nucleic Acids Res*. **37**:W202-8.

Berendzen, K. W., Weiste, C., Wanke, D., Kilian, J., Harter, K., and Dröge-Laser, W. (2012). Bioinformatic cis-element analyses performed in Arabidopsis and rice disclose bZIP- and MYB-related binding sites as potential AuxRE-coupling elements in auxin-mediated transcription. *BMC Plant Biol*. **12**:125.

Berg, O. G., and von Hippel, P. H. (1987). Selection of DNA binding sites by regulatory proteins. Statistical-mechanical theory and application to operators and promoters. *J. Mol. Biol*. **193**:723–50.

Boer, D. R., Freire-Rios, A., van den Berg, W. a M., Saaki, T., Manfield, I. W., Kepinski, S., López-Vidrieo, I., Franco-Zorrilla, J. M., de Vries, S. C., Solano, R., et al. (2014). Structural basis for DNA binding specificity by the auxin-dependent ARF transcription factors. *Cell* **156**:577–589.

Bulyk, M. L. (2002). Nucleotides of transcription factor binding sites exert interdependent effects on the binding affinities of transcription factors. *Nucleic*

496 *Acids Res*. **30**:1255–1261.
497 **Cherenkov, P., Novikova, D., Omelyanchuk, N., Levitsky, V., Grosse, I., Weijers,**
498 **D., and Mironova, V.** (2018). Diversity of cis-regulatory elements associated
499 with auxin response in Arabidopsis thaliana. *J. Exp. Bot*. **69**:329–339.
500 **Dinesh, D. C., Villalobos, L. I. A. C., and Abel, S.** (2016). Structural Biology of
501 Nuclear Auxin Action. *Trends Plant Sci*. **21**:302–316.
502 **Finet, C., Berne-Dedieu, A., Scutt, C. P., and Marlétaz, F.** (2013). Evolution of the
503 ARF Gene Family in Land Plants: Old Domains, New Tricks. *Mol. Biol. Evol*.
504 **30**:45–56.
505 **Franco-Zorrilla, J. M., López-Vidriero, I., Carrasco, J. L., Godoy, M., Vera, P.,**
506 **and Solano, R.** (2014). DNA-binding specificities of plant transcription factors
507 and their potential to define target genes. *Proc. Natl. Acad. Sci. U. S. A*.
508 **111**:2367–2372.
509 **Guilfoyle, T., Hagen, G., Ulmasov, T., and Murfett, J.** (1998). How does auxin turn
510 on genes? *Plant Physiol*. **118**:341–347.
511 **Han, M., Park, Y., Kim, I., Kim, E. H., Yu, T. K., Rhee, S., and Suh, J. Y.** (2014).
512 Structural basis for the auxin-induced transcriptional regulation by Aux/IAA17.
513 *Proc. Natl. Acad. Sci. U. S. A*. **111**:18613–18618.
514 **Hanley, J. A., and McNeil, B. J.** (1982). Maximum attainable discrimination and the
515 utilization of radiologic examinations. *J. Chronic Dis*. **35**:601–611.
516 **Keilwagen, J., Grau, J., Paponov, I. A., Posch, S., Strickert, M., and Grosse, I.**
517 (2011). De-novo discovery of differentially abundant transcription factor binding
518 sites including their positional preference. *PLoS Comput. Biol*. **7**.
519 **Kim, S., Brostromer, E., Xing, D., Jin, J., Chong, S., Ge, H., Wang, S., Gu, C.,**
520 **Yang, L., Gao, Y. Q., et al.** (2013). Probing Allostery Through DNA. *Science*
521 *(80-.)*. **339**:816–819.
522 **Korasick, D. A., Westfall, C. S., Lee, S. G., Nanao, M. H., Dumas, R., Hagen, G.,**
523 **Guilfoyle, T. J., Jez, J. M., and Strader, L. C.** (2014). Molecular basis for
524 AUXIN RESPONSE FACTOR protein interaction and the control of auxin
525 response repression. *Proc. Natl. Acad. Sci. U. S. A*. **111**:5427–5432.
526 **Korasick, D. A., Chatterjee, S., Tonelli, M., Dashti, H., Lee, S. G., Westfall, C. S.,**
527 **Fulton, D. B., Andreotti, A. H., Amarasinghe, G. K., Strader, L. C., et al.**
528 (2015). Defining a two-pronged structural model for PB1 domain interaction in

529 plant auxin responses. *J. Biol. Chem.* **290**:12868–12878.
530 **Lavy, M., and Estelle, M.** (2016). Mechanisms of auxin signaling. *Development*
531 **143**:3226–3229.
532 **Leyser, O.** (2018). Auxin Signaling. *Plant Physiol.* **176**:465–479.
533 **Liao, C.-Y., Smet, W., Brunoud, G., Yoshida, S., Vernoux, T., and Weijers, D.**
534 (2015). Reporters for sensitive and quantitative measurement of auxin response.
535 *Nat. Methods* **12**:207–210.
536 **Mathelier, A., and Wasserman, W. W.** (2013). The next generation of transcription
537 factor binding site prediction. *PLoS Comput Biol* **9**:e1003214.
538 **Medina-Rivera, A., Defrance, M., Sand, O., Herrmann, C., Castro-Mondragon,**
539 **J. A., Delerce, J., Jaeger, S., Blanchet, C., Vincens, P., Caron, C., et al.**
540 (2015). RSAT 2015: Regulatory Sequence Analysis Tools. *Nucleic Acids Res.*
541 **43**:W50–W56.
542 **Mironova, V. V., Omelyanchuk, N. A., Wiebe, D. S., and Levitsky, V. G.** (2014).
543 Computational analysis of auxin responsive elements in the Arabidopsis thaliana
544 L. genome. *BMC Genomics* **15**:S4.
545 **Mironova, V., Teale, W., Shahriari, M., Dawson, J., and Palme, K.** (2017). The
546 Systems Biology of Auxin in Developing Embryos. *Trends Plant Sci.* **22**:225–
547 235.
548 **Moyroud, E., Minguet, E. G., Ott, F., Yant, L., Posé, D., Monniaux, M., Blanchet,**
549 **S., Bastien, O., Thévenon, E., Weigel, D., et al.** (2011). Prediction of regulatory
550 interactions from genome sequences using a biophysical model for the
551 Arabidopsis LEAFY transcription factor. *Plant Cell* **23**:1293–306.
552 **Nanao, M. H., Vinos-Poyo, T., Brunoud, G., Thévenon, E., Mazzoleni, M., Mast,**
553 **D., Lainé, S., Wang, S., Hagen, G., Li, H., et al.** (2014). Structural basis for
554 oligomerization of auxin transcriptional regulators. *Nat. Commun.* **5**:3617.
555 **O'Malley, R., Huang, S., Song, L., and Lewsey, M.** (2016). Cistrome and
556 epicistrome features shape the regulatory DNA landscape. *Cell* **165**.
557 **Oh, E., Zhu, J. Y., Bai, M. Y., Arenhart, R. A., Sun, Y., and Wang, Z. Y.** (2014).
558 Cell elongation is regulated through a central circuit of interacting transcription
559 factors in the Arabidopsis hypocotyl. *Elife* Advance Access published 2014,
560 doi:10.7554/eLife.03031.
561 **Parcy, F., Vernoux, T., and Dumas, R.** (2016). A Glimpse beyond Structures in

562 Auxin-Dependent Transcription. *Trends Plant Sci*. **21**:574–583.
563 **Pierre-Jerome, E., Moss, B. L., Lanctot, A., Hageman, A., and Nemhauser, J. L.**
564 (2016). Functional analysis of molecular interactions in synthetic auxin response
565 circuits. *Proc. Natl. Acad. Sci. U. S. A.* **113**:11354–11359.
566 **Sayou, C., Nanao, M. H., Jamin, M., Posé, D., Thévenon, E., Grégoire, L.,**
567 **Tichtinsky, G., Denay, G., Ott, F., Peirats Llobet, M., et al.** (2016). A SAM
568 oligomerization domain shapes the genomic binding landscape of the LEAFY
569 transcription factor. *Nat. Commun.* **7**:11222.
570 **Simonini, S., Bencivenga, S., Trick, M., and Østergaard, L.** (2017). Auxin-Induced
571 Modulation of ETTIN Activity Orchestrates Gene Expression in Arabidopsis.
572 *Plant Cell* **29**:1864–1882.
573 **Ulmasov, T., Liu, Z. B., Hagen, G., and Guilfoyle, T. J.** (1995). Composite
574 structure of auxin response elements. *Plant Cell* **7**:1611–1623.
575 **Ulmasov, T., Murfett, J., Hagen, G., and Guilfoyle, T. J.** (1997). Aux/IAA proteins
576 repress expression of reporter genes containing natural and highly active
577 synthetic auxin response elements. *Plant Cell* **9**:1963–71.
578 **Vernoux, T., Brunoud, G., Farcot, E., Morin, V., Van den Daele, H., Legrand, J.,**
579 **Oliva, M., Das, P., Larrieu, A., Wells, D., et al.** (2014). The auxin signalling
580 network translates dynamic input into robust patterning at the shoot apex. *Mol.*
581 *Syst. Biol.* **7**:508.
582 **Wasserman, W. W., and Sandelin, A.** (2004). Applied bioinformatics for the
583 identification of regulatory elements. *Nat. Rev. Genet.* **5**:276–287.
584 **Weijers, D., and Wagner, D.** (2016). Transcriptional Responses to the Auxin
585 Hormone. *Annu. Rev. Plant Biol.* **67**:539–574.
586 **Workman, C. T., Yin, Y., Corcoran, D. L., Ideker, T., Stormo, G. D., and Benos,**
587 **P. V** (2005). enoLOGOS: a versatile web tool for energy normalized sequence
588 logos. *Nucleic Acids Res.* **33**:W389-92.
589 **Zemlyanskaya, E. V., Wiebe, D. S., Omelyanchuk, N. A., Levitsky, V. G., and**
590 **Mironova, V. V.** (2016). Meta-analysis of transcriptome data identified
591 TGTCNN motif variants associated with the response to plant hormone auxin in
592 Arabidopsis thaliana L. *J. Bioinform. Comput. Biol.* **14**:1641009.
593 **Zhao, Y., Ruan, S., Pandey, M., and Stormo, G. D.** (2012). Improved Models for
594 Transcription Factor Binding Site Identification Using Nonindependent

Interactions. *Genetics* **191**:781–790.

TABLE AND FIGURES LEGENDS

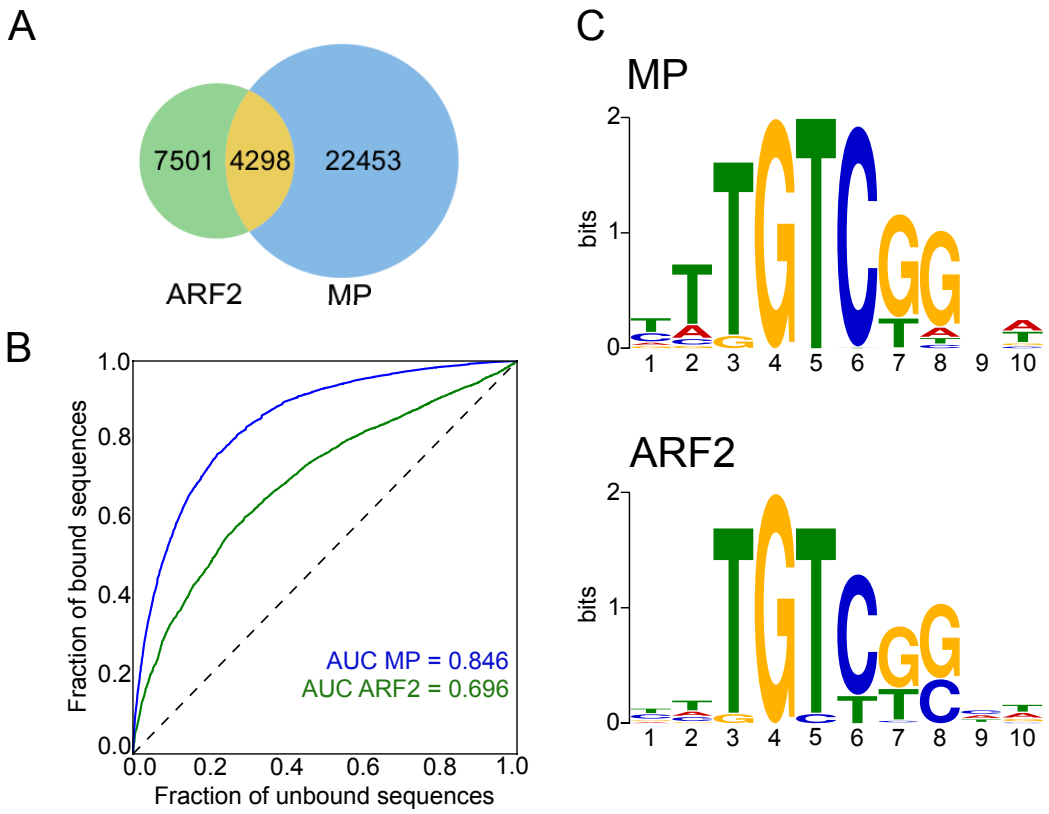

Figure 1: (**A**) Venn diagram of regions bound by ARF2 or MP in DAP-seq. (**B**) ROC curves and AUC values for MP and ARF2 PWM models. (**C**) Logo for MP and ARF2 PWM.

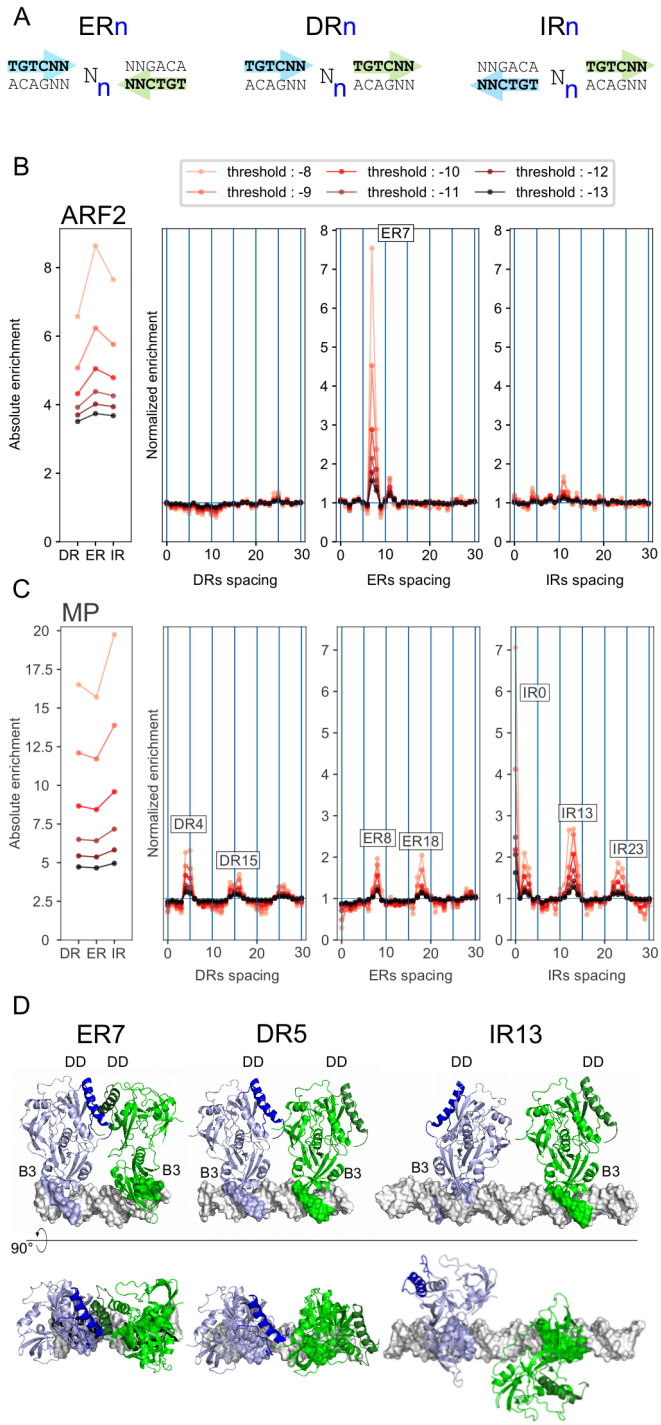

Figure 2: ARFbs configurations enrichment. (A) Definition of ERn, DRn and IRn. (B-C) Over-representation of dimeric ARFbs configurations in DAP-seq regions compared to an unbound set of sequences generated for ARF2 (B) and MP (C). The left panels quantify the absolute enrichment for all ERn, DRn and IRn (0≤n≤30) as compared to the background set. Right panels present the normalized enrichment for each ERn, DRn and IRn (see Methods). **(D)** Structural modelling of DR5 and IR13 ARF complexes based on ER7 ARF1 structure (PDB entry 4LDX) (Boer et al., 2014).

612 Note the dimerization interface present on ER7 is absent in the two other
613 configurations.

614

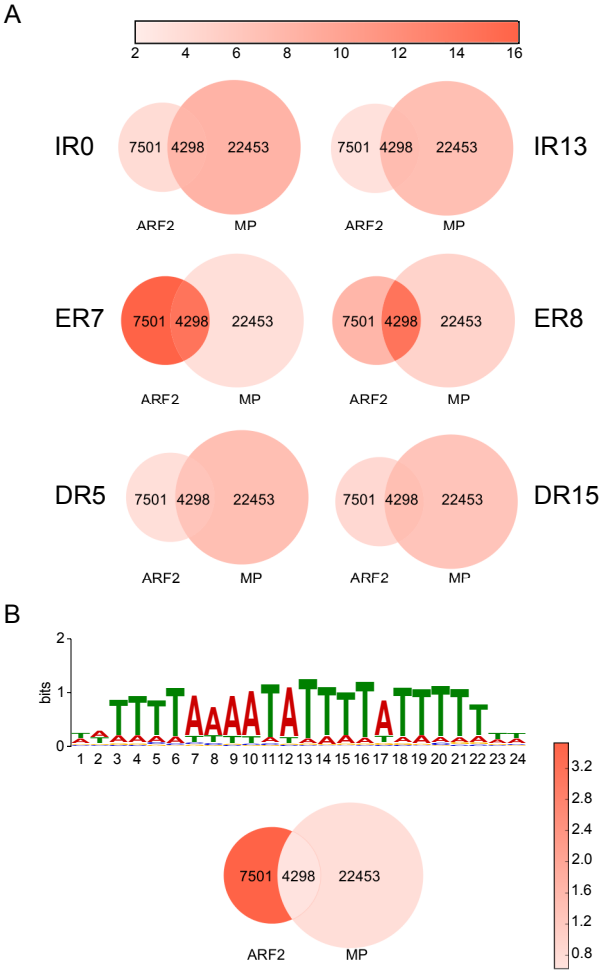

Figure 3: (A) Venn diagrams coloured according to the frequency (in %) of a few ARFbs conformations in MP-specific, ARF2-specific and MP/ARF2 common regions. (**B**) Fraction of regions containing at least one AT rich motif in MP-specific, ARF2-specific and MP/ARF2 common regions.

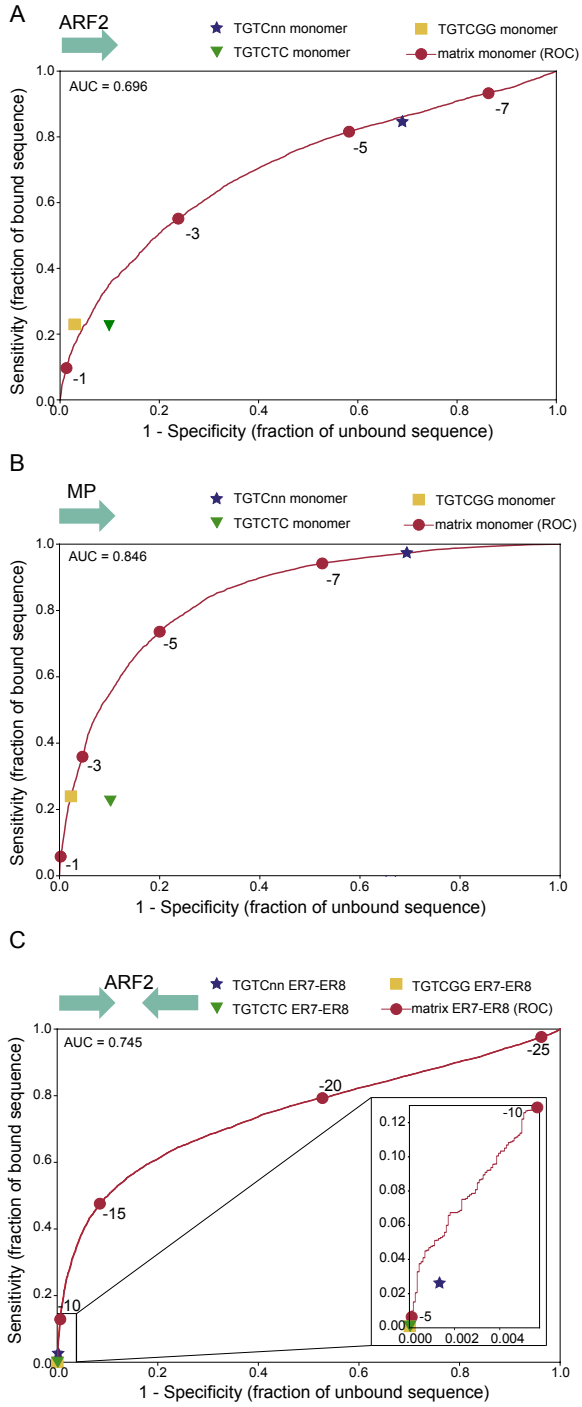

Figure 4: Comparison between PWM and consensus sensitivity and specificity. For all graphs, red dots correspond to score thresholds used to plot the PWM ROC curves. For consensus search, a sequence is considered positive for TGTC, TGTCGG or TGTCTC if this sequence is present at least once in the DNA region. The ER7-8 models were built as described in methods (**A**) ARF2 PWM and consensus on ARF2 bound regions. (**B**) MP PWM and consensus on MP bound regions. (**C**) ER7-8 PWM and consensus models on ARF2 bound regions.

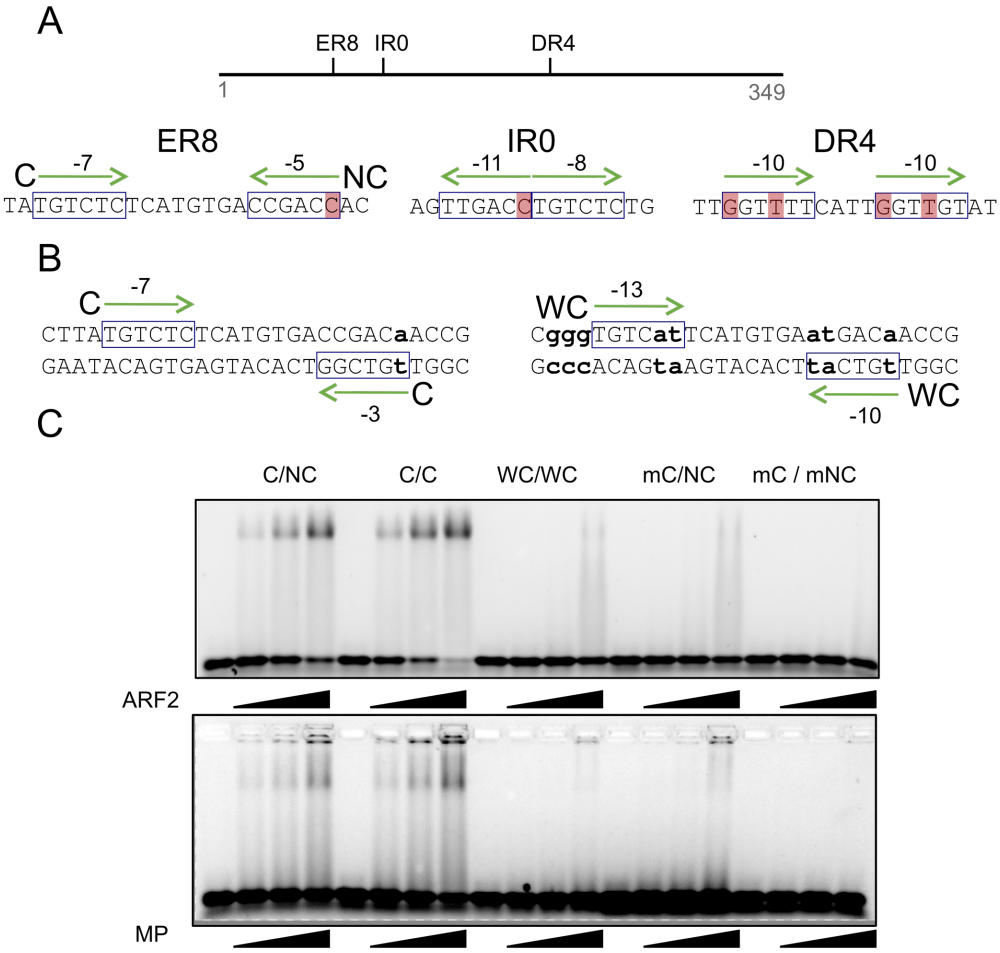

Figure 5: (A) Arabidopsis *IAA19* promoter with position, sequence and scores of ARFbs. (B) ER8 and its variants used in EMSA. (**C**) EMSA using ARF2 and MP proteins on probes described in B and two mutant probe controls with one (mC) or two mC/mNC sides of the ER8 mutated. ARF2 and MP are used at increasing concentrations: 0, 125, 250 and 500 nM. Colour shading indicates difference from consensus.

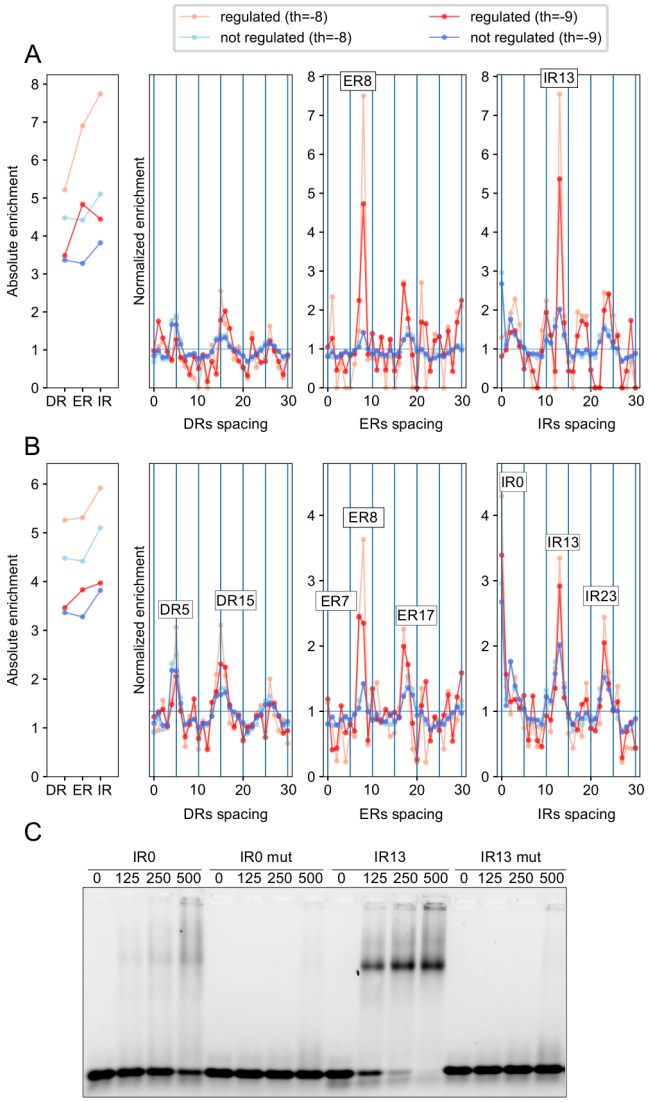

637

638 **Figure 6**: Spacing enrichment in promoter regions bound by MP were analysed in auxin
639 up-regulated very high-confidence (**A**) or high-confidence genes (B) (red colours) and
640 non-auxin-regulated genes (**B**) (blue colours) at two different score thresholds. The
641 enrichment of ER7/8 and IR13 is increased for genes of the very high confidence auxin
642 upregulated gene list. (C) EMSA showing the binding of MP to IR0 and IR13 motifs
643 and the corresponding control mutant probes. MP is used at increasing concentrations:
644 0, 125, 250 and 500 nM.

645

646

647

648 **SUPPLEMENTAL INFORMATION**

649 Supplemental Information is available at Molecular Plant Online.

650

651 **Supplemental data**

652

653 **This file contains**

654

655 **5 Supplemental figures**

656 **1 Supplemental table**

657

658

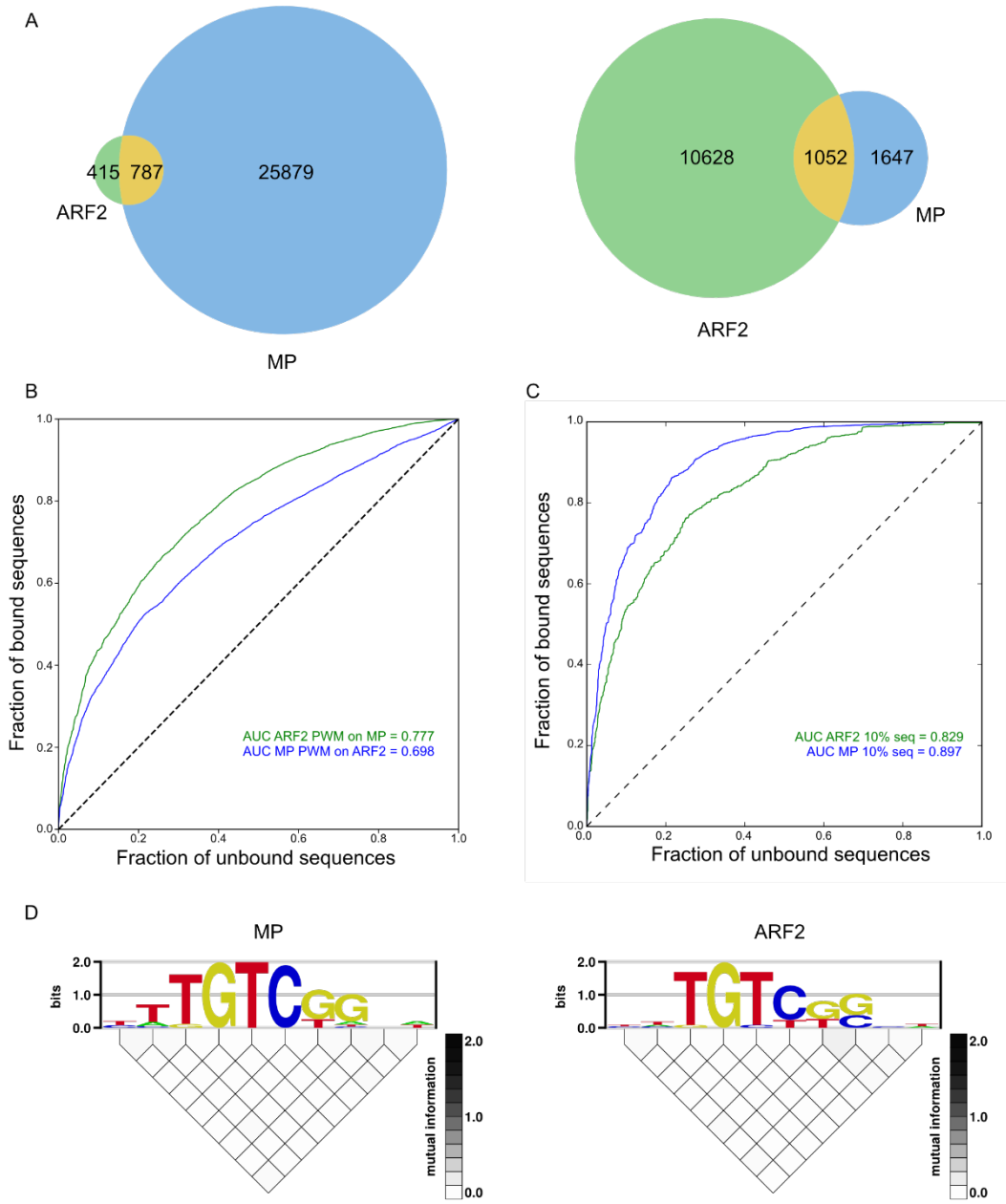

Supplemental Figure 1: **(A)** 2 Venn diagrams with the 10% top bound regions for ARF2 against all MP regions and the 10% top bound regions for MP against all ARF2 regions. This shows that there are regions specifically bound by a single factor even in the highest confidence regions **(B-C)** ROC curves with ARF2 PWM on MP bound regions and MP PWM on ARF2 regions. AUROC value decrease slightly as compared to Figure 1 **(D)** Enologos analysis of MP and ARF2 motifs (1). No dependency between nucleotide position is detected.

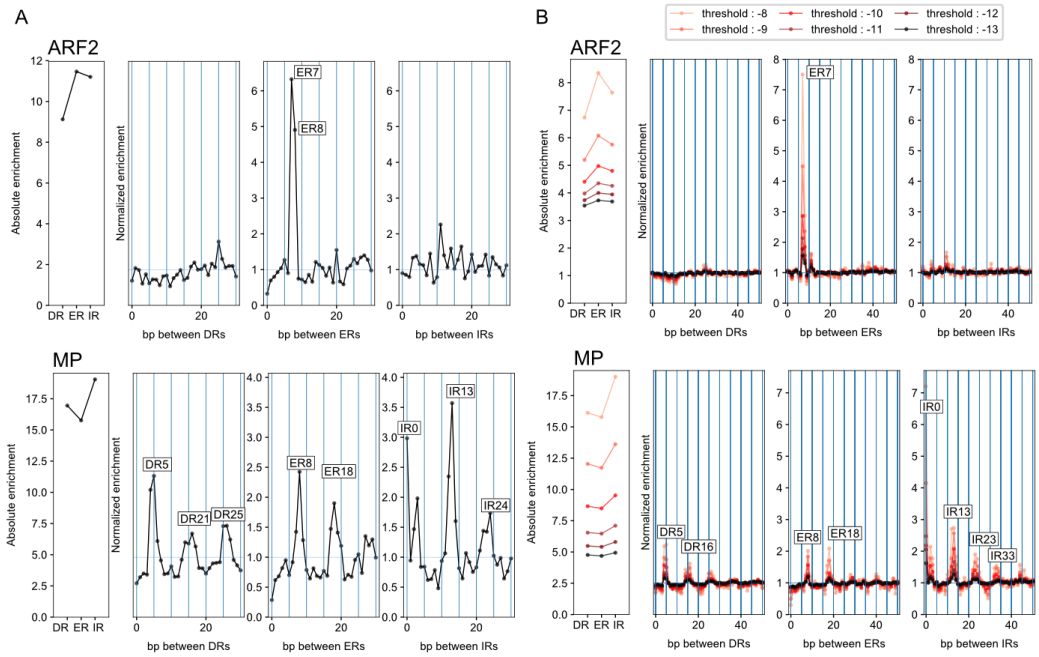

668 **Supplemental Figure 2**: **(A)** Enrichment of spacings between TGTC **(B)** Spacing
669 enrichment for DRn, ERn and IRn for 0≤n≤50. Threshold indicates the PWM score
670 threshold value used for ARFbs detection

671

672

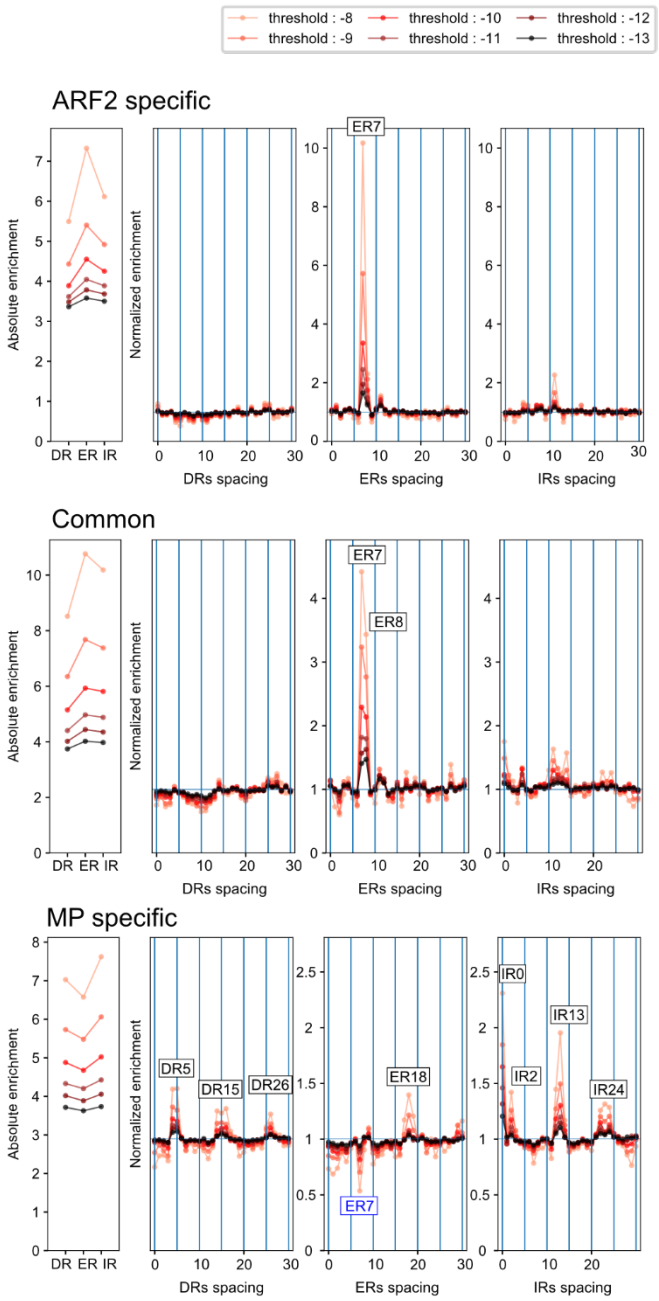

673

674

675 **Supplemental Figure 3:** Spacing enrichment in MP-specific, ARF2-specific and
676 MP/ARF2 common regions, compared to unbound sets of sequences. Threshold
677 indicates the PWM score threshold value used for ARFbs detection. Note ER7 is
678 depleted in MP-specific bound regions.

679

680

681

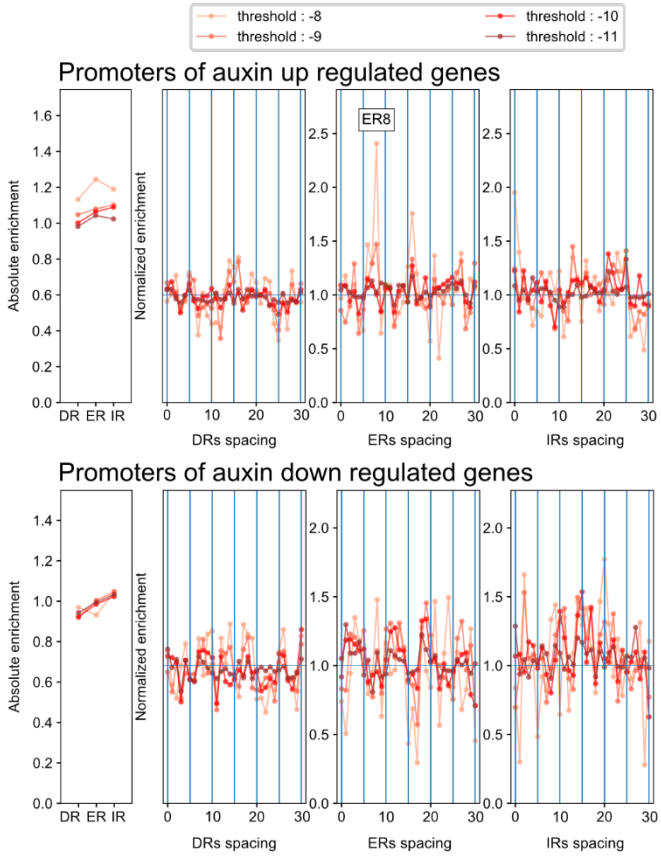

682

683 **Supplemental Figure 4:** ARFbs over-represented conformations in the promoters of
684 the auxin up-regulated genes (upper panel) or the down-regulated genes (lower panel)
685 We used very high and high confidence genes and compared to auxin insensitive gene
686 promoters. Threshold indicates the PWM score threshold value used for ARFbs
687 detection

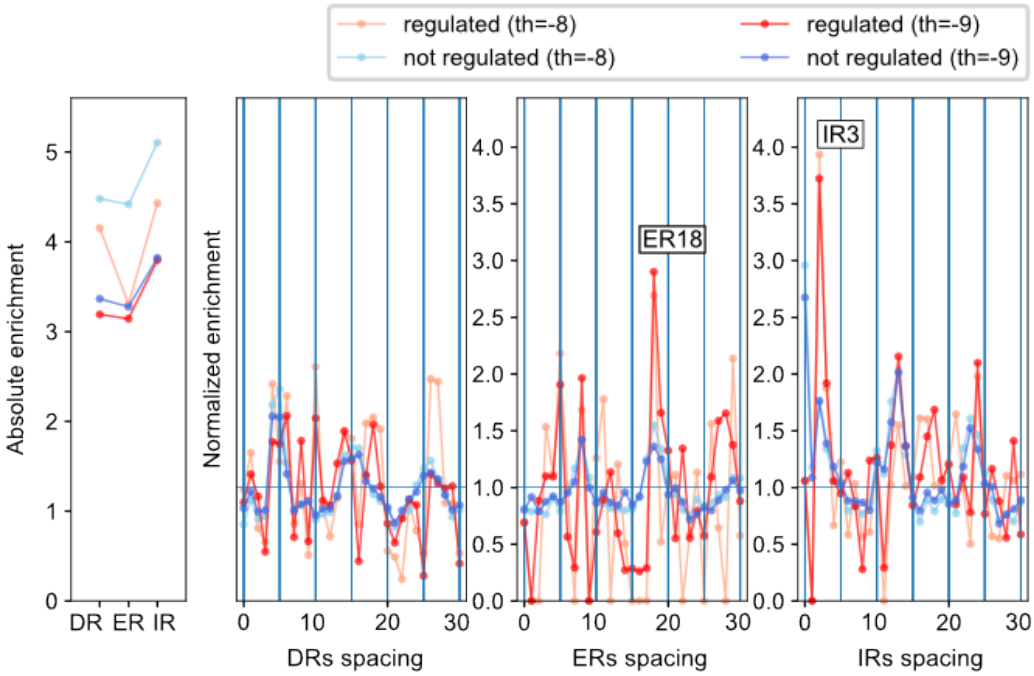

688

689 **Supplemental Figure 5:** Promoter regions bound by MP were analysed in down-
690 regulated (red colours) and non-regulated genes (blue colours) in high confidence gene
691 lists (Supplemental file 1). The regions not bound by MP from auxin insensitive
692 promoters were used as background. Threshold indicates the PWM score threshold
693 value used for ARFbs detection

694

695

696

697

698 **Supplemental Table 1**. Sequences of DNA probes for EMSAs. Bold letters show ARF
699 binding sequence. Lower case letters indicate the nucleotides variation introduced.
700

Oligonucleotide	DNA sequence (5'->3')
ER8 C/NC	GCAAACTTA**TGTCTC**TCATGTGA**CCGACC**ACCGCATC
ER8 C/C	GCAAACTTA**TGTCTC**TCATGTGA**CCGACa**ACCGCATC
ER8 WC/WC	GCAAACggg**TGTCat**TCATGTGA**atGACa**ACCGCATC
ER8 mC/NC	GCAAACTTA**TGTCTC**TCATGTGA**CCGttC**ACCGCATC
ER8 mC/mNC	GCAAACTTA**TaaCTC**TCATGTGA**CCGttC**ACCGCATC
IR0	GATGCAGTCATGTG**CCGACATGTCGG**CATGTGCTCACAT
IR0 mut	GATGCAGTCATGTG**CCGttATaaCGG**CATGTGCTCACAT
IR13	GATGCAG**CCGACA**AAACACATGATTT**TGTCGG**CTCACAT
IR13 mut	GATGCAG**CCGttA**AAACACATGATTT**TaaCGG**CTCACAT

701

702